

Received 20 December 2022, accepted 9 January 2023. Date of publication 00 xxxx 0000, date of current version 00 xxxx 0000.

Digital Object Identifier 10.1109/ACCESS.2023.3238572

A Bioinspired Emergent Control for Smart Grids

AQ:1 **MARCEL SIMEÓN GARCÍA MEDINA**^{1,3}, **JOSE AGUILAR**^{2,3,4,5}, (Member, IEEE),
AND MARIA D. RODRÍGUEZ-MORENO^{2,6}

¹Laboratorio de Prototipos, Universidad Nacional Experimental del Táchira, San Cristóbal 5001, Venezuela

²Escuela Politécnica Superior. ISG. Universidad de Alcalá, 28805 Alcalá de Henares, Spain

³CEMISID, Universidad de Los Andes, Mérida 5101, Venezuela

⁴GIDITIC, Universidad EAFIT, Medellín 50022, Colombia

AQ:2 ⁵IMDEA Networks Institute, Leganés, 28918 Madrid, Spain

AQ:3 ⁶TNO, Intelligent Autonomous Systems Group (IAS), The Hague, The Netherlands

AQ:4 Corresponding author: Jose Aguilar (aguilarjos@gmail.com)

AQ:5 The work of Jose Aguilar was supported by the European Union's Horizon 2020 Research and Innovation Program under the Marie Skłodowska-Curie Grant through GOT ENERGY TALENT under Agreement 754382. The work of Maria D. Rodríguez-Moreno was supported in part by JCLM Project by the European Regional Development Fund (FEDER) under Grant SBPLY/19/180501/000024, and in part by the Spanish Ministry of Science and Innovation Project by FEDER under Grant PID2019-109891RB-I00.

AQ:6 **ABSTRACT** Satisfying energy demand has become a global problem that is on the rise due to population growth, infrastructure deterioration, a decline in fossil fuel sources, and high costs for investment, among others. Smart grids, in addition to those challenges that they have at the level of energy generation, have other management challenges derived from the great diversity of components that make them up, such as energy storage systems (batteries, capacitors, etc.), the different types of consumers (controllable, non-controllable loads) and prosumers (electric vehicles, self-sustaining buildings, micro-grid, etc.), among others. Consequently, a distributed control problem is presented, mainly oriented to the coordination of its components. A possible solution is to achieve the participation of each component when conditions are more favorable, such as prioritizing production with renewable energy sources, or taking advantage of prosumers so that they can meet local demand, among other things. Therefore, new strategies with a distributed approach such as bio-inspired emergent controls are necessary. The objective of this work is the specification of an emergent control approach to coordinate a smart grid. This approach allows the coordination of the energy supply in various operating scenarios. The results obtained demonstrate a perfect synchronization between the different smart grid components (agents), prioritizing renewable energy sources, regardless of the operational context (for example, in cases of failures, unsuitable environmental conditions, etc.).

INDEX TERMS Emergent control, smart grid, bioinspired algorithms, distributed artificial intelligence.

1. INTRODUCTION

In recent years, profound changes have occurred in society in relation to energy systems, highlighting the awareness in energy consumption due to the preservation of the environment [1] and the high costs. This has led users to establish load control mechanisms [2] to manage and prioritize its use (management on the demand side) [3], [4] to save energy. But also, a new role in the energy ecosystems has emerged, that of the prosumer, thanks to the incorporation of renewable energy sources in homes, offices, and industries [5]. Likewise, the energy ecosystem has been extended to other

actors such as electric vehicles (EV), which are capable of producing their own energy from solar panels, or exchanging their surplus when they are parked. All of the above has made energy networks spaces of great intermittence, randomness, and dynamism.

Renewable generation sources such as solar and geothermal energies, among others, take advantage of the potential of natural resources. They become an alternative to avoid or reduce energy from large generation centers (main grid) [6]. The disadvantages of these centers are [7]: high energy losses, high emissions (if based on fossil fuels), excessive use of water (in thermal power plants), hazardous waste generation (if based on nuclear power), expensive infrastructure, fast depletion of fossil fuel, air pollution, and many

The associate editor coordinating the review of this manuscript and approving it for publication was Moussa Ayyash^{1b}.

others. However, the variability of primary sources must be addressed for the renewable generation systems, such as changes in wind speed, daytime cloud cover, or tidal intensity that affect energy conversion [8]. Then, for this, additional components such as energy storage systems (ESS) must be used, which mitigate these fluctuations. But that is not enough, the interconnection of micro-grids (MGs) is necessary to make the system robust, which requires effective coordination mechanisms between the components. The MG control problem in a smart grid is a distributed control problem, mainly oriented to the coordination of its components without a central control that governs them.

The motivation of this work is to adequately integrate and coordinate the various actors in an energy ecosystem, both at the generation and demand level, to meet energy needs, maximizing the use of renewable energy sources, trading with neighboring networks, managing controllable loads according to prioritization levels, charging storage devices only with renewable energy sources, and reducing the energy coming from the main grid. To achieve the above, new distributed strategies are required, such as the one based on emergent control. For example, some bioinspired techniques/models could be used, such as the response threshold model, which is based on the behaviour of ants to respond to environmental stimuli, achieving self-control actions through the use of local variables in a distributed context. The objective of this work is to take advantage of the self-control mechanism of the response threshold model, so that each component of a MG participates in the energy exchange when the conditions are more favorable [38]. For this, it is necessary to identify the local variables and rules for the decision-making, as well as the feedback mechanisms between them, to formulate an emerging control proposal that allows efficient energy management. This work differs from previous ones in the use of a bioinspired emergent control strategy that allows coordination at the micro level. The main contributions of our work are:

- The definition of an approach for the coordination and distributed control problems. The original RTM was used to solve the task assignment problem.
- The definition of a procedure to deploy various distributed energy resources (DER) in a MG through the use of the response threshold model.
- The definition of a distributed mechanism to prioritize the use of renewable sources through the formulation of local decision rules.

This article is organized as follows: Section I presents the related works; Section II describes the theoretical framework around the proposed emerging technique and the process to be controlled. Section III presents our bioinspired emergent control strategy based on the response threshold model. Section IV describes the experiments carried out, the discussion of the results, and the comparison with other works. Finally, the last section presents the conclusions and future works.

II. RELATED WORK

From the first works in the multi-MGs (MMGs) concept, Nikmehr and Najafi Ravadanegh [9] discussed the distribution network operation. The economic operation of MMGs is formulated as an optimization problem, with a stochastic modelled of both small-scale energy resources (SSERs) and load demand at each MG. Bandejas et al. [10] addressed energy trading among multiple MGs for different energy markets to facilitate energy trading among prosumers, producers and customers. Finally, a case study is presented to evaluate the cooperation among five industrial MGs. Yassine et al. [11] proposed some distributed control schemes for MG control.

Abhishek et al. [12] presented a review of hierarchical control strategies that provide control for a MG. Also, the advantages and limitations of these control strategies are discussed in this study. In [13], Ahmethodzic et al. presented a literature review of MG control architectures. Likewise, they describe their main features of them and their positive and negative sides. Sen and Kumar [14] provided a comprehensive survey of different control aspects for MGs, with a classification based on four control strategies: centralized, decentralized, distributed and hierarchical. Also, the principles behind, their applicability and performances are presented.

Palensky and Dietrich [16] proposed a load planning approach dependent on gauge power costs and pre-booked burdens. Aguilar et al. [15] set a scheduling system that automatically generated hours of use of the controllable load appliances in a home, in such a way that the use of renewable energy is maximized. To achieve this, they define an autonomous cycle of data analysis tasks composed of three tasks, two tasks for estimating the renewable energy produced (supply) and the required load (demand), coupled with a scheduling task to generate the plans of use of appliances.

Touma et al. [17] reviewed demand-side management systems, particularly pricing techniques, as a part of a control system of MGs. They identified shortcomings in current researches concerning demand-side management and highlighted future research horizons. In the work of Abou El-Ela et al. [18], a fuzzy logic controller (FLC) system is proposed to decide the charging/discharging priority level of each EV based on the state-of-charge (SOC) level of its battery. Mathur et al. [19] presented different technologies available for EV integration in the MG community. This work also discusses the necessity of vehicle charging stations to meet the technical requirements of the EV.

In [38], Alagoz et al. introduce the concept of an emergent controller applied to smart grids, as an intelligent control-communication unit (SCCUs), whose function is to switch the end-user mode between consumer or producer. Thus, in their case study, the flow of energy can be controlled in both directions to export or import the energy. Particularly, the authors focused on smart grids, and the presented methodology on energy balance and energy balance-oriented flow mechanisms could be useful in the analysis of other complex networks involving uncertainty and variability, such

as biological or social networks. However, the work does not present the possible intelligent algorithms that can be applied to an SCCU.

Finally, Aguilar et al. [20] presented a systematic review of the literature on recent research about energy management systems for smart buildings using artificial intelligence techniques. They focused on autonomous management systems and identified that many types of research are in the domain of decision-making (a large majority on optimization and control tasks), and defined potential projects related to the development of autonomous cycles of data analysis tasks [21], feature engineering [22], or multi-agent systems [23], among others. As can be seen from recent previous works, there are no proposals linked to using distributed control approaches based on bio-inspired techniques, which allow the emergence of coordination processes between the components of a smart grid. In that sense, this proposal focuses on this field of study.

III. THEORETICAL FRAMEWORK

This section presents the bioinspired algorithm used in this work, the response threshold model, as well as the components of the smart grid that will be modeled.

A. RESPONSE THRESHOLD MODEL (RTM)

This model emulates the reaction of ants to the pheromone intensity (external/internal stimuli) according to the behavior of the division of labor in ant colonies [24]. In this way, the colonies can adapt to changing environments. For instance, ants can have different behaviors depending on their distance from the nest and their abilities for a given task [25]. The reaction to external/internal stimuli can be modeled using a response threshold (θ). Thus, an ant with a low response threshold can be a worker with high probability; and with a high response threshold, it is not a worker, even if external stimuli are high [24]. In a classical RTM, the probability q for an agent works is defined by:

$$q_j(t) = \frac{s_j(t)^2}{s_j(t)^2 + \theta_{ij}(t)^2} \quad (1)$$

where θ_{ij} denotes the response threshold of the ant i to perform task j at time t , and s_j is the external/internal stimulus. On the other hand, the ants modify the intensity of the stimulus (s_j) according to equation (2), as a way of exerting control over the system through an individual or collective learning process, by linking rewards to stimuli [15].

$$s_j(t+1) = s_j(t) + \delta - \frac{\alpha N_{act}}{N} \quad (2)$$

In a classical RTM, the intensity of the stimulus depends on the execution of the task. N_{act} is the number of active individuals, N is the number of individuals in the colony, α is a scale efficiency factor to perform the task, and δ is to increase the intensity of the stimulus per unit of time [17]. Also, the response threshold increases when the corresponding task is not performed and decreases when it is performed [24]

according to the next equation:

$$\theta_{ij}(t+1) = \theta_{ij}(t) - y_{ij}\beta\Delta t + (1 - y_{ij})\gamma\Delta t \quad (3)$$

where, y_{ij} is the fraction of individuals of type i doing task j , β is the learning rate, and γ is the forgetting rate. Equation (3) specifies that in the next Δt time units, y_{ij} individuals of type i will do task j , and the rest $(1 - y_{ij})$ something else or nothing [27], [28]. In this way, the RTM models the possibility of reacting to respond to the problem of division of labor in a colony. That combined reinforcement process generates specialized workers in specific tasks.

B. MICROGRIDS (MGs)

A Smart Grid is an energy network that integrates the behaviour and actions of all users connected to it (consumers, providers and prosumers) to ensure an efficient sustainable energy system. A smart grid requires innovative services and products for smart self-monitoring, self-control, and self-healing processes. A MG is a local energy grid with specific elements, acting as a single and controllable entity. It operates in a smart grid but can also operate in island mode. This is the basic element of a smart grid to model. MGs can sell excess power (prosumers) to other grids. In a MG with a non-renewable generation, some of the possible components are diesel engines (DEs), microturbines (MTs), fuel cells (FCs), and combined heat and power (CHP) plants, and a MG with renewable generation includes solar photovoltaic panels (PV) and wind turbines (WTs), among other elements [9]. In this work, we are interested in PV, WT, ESS, EV, external sources like utility grids, synchronous generators (SG) as hydroelectric sources, and demand side control (controllable and uncontrollable loads).

1) PHOTOVOLTAIC SYSTEM (PV)

It is defined as a set of cells connected to provide voltage/current using a photovoltaic panel. The power output of the PV (P_{PV}) depends on solar radiation (see Eq. 4). Therefore, a control strategy is necessary to obtain maximum power production [7]. The maximum energy output of a PV is:

$$P_{PVmax} = \eta S \phi [1 - 0.005(T_a + 25)] \quad (4)$$

where: S is the area of the PV array (m^2), ϕ is the Solar radiation (kW/m^2), T_a is the ambient temperature (e.g., in $^\circ C$) and η is the conversion efficiency of the PV system.

2) WIND TURBINES (WT)

The production of energy of a wind turbine generator depends on wind speed V_W . The wind speed is considered to be the algebraic sum of base wind speed (V_{WB}), gust wind speed (V_{WG}), ramp wind speed (V_{WR}) and noise wind speed (V_{WN}), given by [29]:

$$V_W = V_{WB} + V_{WG} + V_{WR} + V_{WN} \quad (5)$$

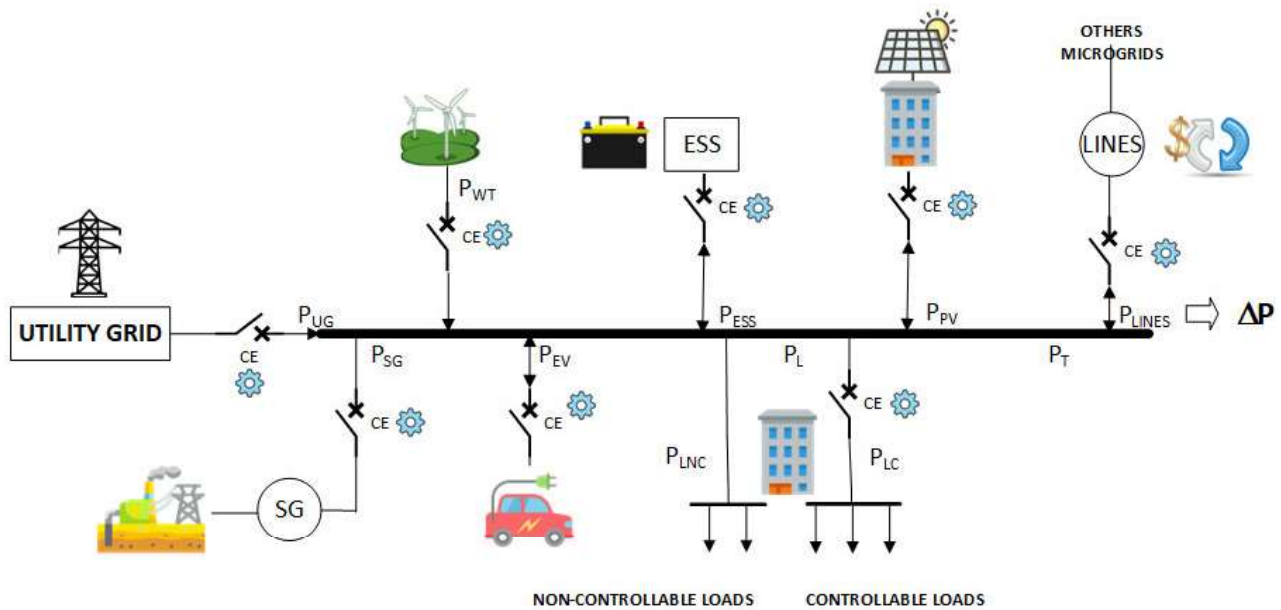


FIGURE 1. Distributed control architecture for a MG.

248 The mechanical power output of the wind turbine is formu-
249 lated as [30]:

$$250 \quad P_{Wmax} = \frac{1}{2} \rho A_r C_p V_w^3 \quad (6)$$

251 where ρ is the air density (kg/m^3), A_r is the swept area of the
252 blade (m^2) and C_p is the power coefficient which is a function
253 of tip speed ratio (λ) and blade pitch angle (β).

254 3) ENERGY STORAGE SYSTEM (ESS)

255 ESS like batteries is one of the most common devices used for
256 saving electrical energy in various applications. Batteries are
257 a backup for WT or PV systems. They are used to store excess
258 energy captured from wind or solar power during windy or
259 sunny days, and also to release stored energy during times
260 of generation shortages. In the field of battery modeling,
261 various models have been proposed [31]. For this work,
262 we use the next modified simple battery model, considering
263 the power [W] instead of voltage [V]:

$$264 \quad V_t = V_{OC} - \left(R_{int} + \frac{K}{SOC} \right) I \quad (7)$$

265 where V_t is the terminal voltage of the battery, I is the
266 discharge current, R_{int} is the battery terminal resistance, K
267 is a polarization constant, and V_{oc} is the open circuit voltage.

268 4) GEOTHERMAL ENERGY PLANTS (GEO)

269 Geothermal energy (GE) is a non-carbon source of renewable
270 energy based on heat flux from the earth's core; a reliable
271 and abundant energy source [32]. In [33], Zarrouk and Moon
272 defined its power generation based on the operating temper-
273 ature and the produced power. The active power output in a

generating unit is given by:

$$274 \quad P_{GEOmax} = \frac{(0.18T_{in} - 10) ATP}{278} \quad (8)$$

275 where, T_{in} is the inlet temperature of the primary
276 (geothermal) fluid ($^{\circ}C$), and ATP is the available thermal
277 power (kW).
278

279 5) PROSUMERS

280 It is an energy user who generates renewable energy in his/her
281 domestic environment, and either stores the surplus energy
282 for future use or trades it to interested energy customers in a
283 smart grid [34]. In general, the objective of the prosumers is to
284 produce and consume energy, as well as share and redistribute
285 excess energy to other users in the grid.

286 6) UTILITY GRID (UG)

287 Main grid or utility grid are equivalent terms, and means a
288 national integrated power delivery system that transmits and
289 delivers energy to consumers at any voltage level. It consists
290 of three main components [35], i) power plants that pro-
291 duce energy from fossil fuels (coal, natural gas, biomass) or
292 non-fossil fuels (wind, solar, nuclear, hydro); ii) transmission
293 lines that carry energy from generating plants to the demand
294 centers; and iii) the transformers that reduce the voltage so
295 that the distribution lines can deliver energy to the final
296 consumer.

297 IV. DESIGN OF A BIOINSPIRED EMERGENT CONTROL SYSTEM

298 In this section, we present the components that we will con-
299 sider in a MG, and its emergent control model. Specifically,
300 the local emergent controllers of each of the agents that make
301

up the MG will be presented. Initially, we describe the process followed for the design of the system.

A. SYSTEM DESIGN PROCESS

In this section, the design of the emergent controller based on the RTM is explained using the methodology MASINA (MultiAgent Systems for INtegrated Automation) [39], [40]. The steps followed in the design are the following:

- Step 1: It defines the agents in the distributed system, with their interactions, states, environment, variables, parameters and behaviors. The complexity of the model will depend on the number of agents and their variables.
- Step 2: This step analyzes and preprocesses the variables of each agent to describe the behavior of the agents, and maybe, their relationships. This may involve converting them to the same dimensions or dimensionless, among other things.
- Step 3: In this step is defined the self-control mechanism based on RTM for each agent. The main objective is to determine the stimulus and threshold of each agent, in order to introduce the reinforcement learning process implicit in the RTM. Also, it defines the feedback mechanisms between the agents.
- Step 4: It defines the activation probability of each agent based on the RTM, for which it uses the stimulus and threshold previously defined. It is the rule for the decision-making of each agent on whether to activate or not.

In summary, the first step is to identify the local variables, and then, the feedback mechanisms between them, as well as the rules for the decision-making of each agent. Specifically, its main variables, the stimulus and the threshold, induce each agent to act or not. The stimulus considers the context information and the threshold is related to the achievement of the objectives. Both use a reinforcement learning process as a self-control mechanism to regulate the agent's response, allowing autonomous coordination actions.

B. ARCHITECTURE OF A MG

This section presents a MG composed of WT, EV, buildings, PV, ESS and external generation sources such as utility grids. They are the agents of our distributed system that describes a MG. Their interactions are defined in Figure 1. All of the above describe the aspects considered in step 1 of our design process.

In general, MG requires a mechanism to guarantee coordinated control actions in order to satisfy the demand. The general system variables required for self-control by the agents are the following.

The total power (P_T) in the MG is represented by the sum of the renewable and non-renewable generation sources and the various types of prosumers. In addition, the loads (P_L) are of two types: controllable and non-controllable (priority) loads; which allows establishing the power differential to determine the excess or deficit of energy in the MG, expressed

through the following equation:

$$\Delta P = P_T - P_L \quad (9)$$

where, P_T is the generated power (see Eq. 10) by the renewable systems (P_H) like WT, PV, among others (see Eq. 11), energy storage systems (P_{ESS}), synchronous generators represented by the geothermal plant (P_{GEO}), non-renewable or large-scale systems such as UG (P_{UG}), and the various types of prosumers such as EV (P_{EV}), self-sustaining buildings, exchange components with other MGs (P_{LINES}).

$$P_T = (P_H + P_{ESS}) + P_{GEO} + P_{UG} + P_{EV} + P_{LINES} \quad (10)$$

$$P_H = P_{WT} + P_{PV} \quad (11)$$

Also, the loads will be divided into controllable (P_{LC}) and non-controllable (P_{LNC}) loads for the purposes of this work (see Eq. 12):

$$P_L = P_{LC} + P_{LNC} \quad (12)$$

Finally, the exchange prosumer with other nodes P_{LINE} is represented by the power differential ΔP of Eq. 9 since it will allow the trading (purchase/sale) of surplus energy with neighbouring MGs. In this work, only one will be considered, but several will be considered in future works such that different negotiation strategies will be necessary, which are beyond the scope of this work. Thus, Eq. 13 represents the surplus energy available in the MG.

$$P_{LINE} = \Delta P \quad (13)$$

C. EMERGENT CONTROL SYSTEM FOR THE MG

In this section, the control model of each agent will be designed, which will be based on RTM, identifying the context variables to update the stimulus and the threshold. Fig. 1 defines the next agents: A PV agent represents the control mechanism to activate or deactivate the energy coming from solar radiation, and the WT agent represents the control mechanism to activate or deactivate the energy from the wind speed. The synchronous generation agent represents a geothermal power plant. The agent of the public network is the one that allows the supply of energy from non-renewable sources such as gas, and oil, among others. They are reserve producers that compensate for the energy demand when storage systems and/or renewable generation fail. The agent of the ESS represents the charge and discharge control processes of the batteries. This agent stores energy during renewable surpluses and releases it during peak load demand. On the other hand, EV agents impose conditions of randomness in demand and production possibilities, sustainable building agents have their own renewable sources and ESSs, and finally, the exchange agent can buy or sell the surpluses in the MG. Below, we present the design of the agents according to the steps described in section IV-A.

1) PHOTOVOLTAIC AGENT

In steps 1 and 2 of the design process, we identify and analyse the variables, context, and dynamics of this agent:

- Behaviour: This agent will be activated when its stimulus tends to increase, which occurs when there is solar radiation (P_{PVmax}), demand (P_L) and there is no energy stored in the batteries ($1 - Soc$) Q_{CAP} . In addition, it is necessary that θ decreases because the power delivered to the electrical network is not covered by renewable energies ($\beta_{PV} \left(1 - \frac{P_H}{P_L}\right) > 0$ and $\gamma_{PV} \frac{P_H}{P_L} \cong 0$). Otherwise, the threshold will increase ($\gamma_{PV} \frac{P_H}{P_L} > 0$), causing the controller to turn off. Thus, the RTM, in the context of the PV agent,.
- Environment: Solar radiation and climatic conditions.
- External variables: Demand and status/capacity of the ESS (battery).
- Internal variables: Conversion efficiency and solar panel area.

In steps 3 and 4, we define the self-control mechanism and the activation probability of this agent based on the RTM. Thus, the RTM, in the context of the PV agent, for an emergent control scheme, is as follows:

$$s_{PV}(t+1) = s_{PV}(t) + w_{PV} (P_{PVmax}(P_L + (1 - Soc) Q_{CAP})) \quad (14)$$

$$\theta_{PV}(t+1) = \theta_{PV}(t) - \beta_{PV} \left(1 - \frac{P_H}{P_L}\right) \Delta t + \gamma_{PV} \frac{P_H}{P_L} \Delta t \quad (15)$$

$$q_{PV}(t) = \frac{s_{PV}(t)^2}{s_{PV}(t)^2 + \theta_{PV}(t)^2}, \quad (16)$$

where, w_{PV} is an attenuation factor to make the variations of the perceived signals less sensitive, P_{PVmax} is the maximum power output of the PV according to solar radiation (see Eq. 4), $(1 - Soc)$. (state of charge) is the percent of available capacity of a battery ($0 < Soc < 1$), Q_{CAP} is the maximum energy capacity of the battery [kW], and P_{PV} is the power supplied by the solar panel.

Specifically, Eq. 16 is the probability that the PV agent generates energy, Eq. 14 is the intensity of the stimulus for the same agent, and its response threshold is updated according to Eq. 15.

2) WIND GENERATION AGENT

Steps 1 and 2 of the design process identify and specify the variables, context, and dynamics of this agent:

- Behaviour: This agent will be activated when the stimulus tends to increase, which occurs when there is wind speed (P_{Wmax}), demand (P_L) and there is no energy stored in the batteries ($1 - Soc$) Q_{CAP} . In addition, it is necessary that θ decreases because the power delivered to the electrical network is not covered by renewable energies ($\beta_{WT} \left(1 - \frac{P_H}{P_L}\right) > 0$ and $\gamma_{WT} \frac{P_H}{P_L} \cong 0$). Otherwise, the threshold will increase ($\gamma_{WT} \frac{P_H}{P_L} > 0$), causing the controller to turn off.
- Environment: wind speed and climatic conditions.

- External variables: Demand and status/capacity of the ESS (battery).
- Internal variables or parameters: Conversion efficiency, air density and swept area of the blade.

Steps 3 and 4 define the self-control mechanism and the activation probability of this agent based on the RTM. Thus, the RTM in the context of the WT agent, for an emergent control scheme, is as follows:

$$s_{WT}(t+1) = s_{WT}(t) + w_{WT} (P_{Wmax}(P_L + (1 - Soc) Q_{CAP})) \quad (17)$$

$$\theta_{WT}(t+1) = \theta_{WT}(t) - \beta_{WT} \left(1 - \frac{P_H}{P_L}\right) \Delta t + \gamma_{WT} \frac{P_H}{P_L} \Delta t \quad (18)$$

$$q_{WT}(t) = \frac{s_{WT}(t)^2}{s_{WT}(t)^2 + \theta_{WT}(t)^2}, \quad (19)$$

where, w_{WT} is an attenuation factor to make the variations of the perceived signals less sensitive, P_{WTmax} is the maximum power output of the wind turbine that varies according to wind speed (see Eq. 6), and P_{WT} is the power supplied by the wind turbine to the electrical grid according to demand.

Specifically, Eq. 19 is the probability that the WT agent generates energy, Eq. 17 is the intensity of the stimulus for the same agent, and its response threshold is updated according to Eq. 18.

3) ENERGY STORAGE AGENT

The RTM applied to the energy storage agent is presented in this section. This emergent control system must manage three states: as consumer, producer or passive. The equations of this emergent control system for the 3 previous states are as follows:

Producer:

Next, we present steps 1 and 2 of the design process in this agent as a producer:

- Behaviour: It is a producer when the solar or wind potential is not enough to satisfy the demand and it has stored energy.
- Environment: Does not apply
- External variables: Demand and renewable sources.
- Internal variables: SOC.

Steps 3 and 4 define the self-control mechanism and the activation probability based on the RTM of this agent as a producer. Eq. 20 describes the stimulus for production when the demand (P_L) is not covered by renewable energies (P_H) and there is stored energy ($Soc (P_L - P_H) > 0$). On the other hand, the threshold (Eq. 21) is modified according to the energy stored (SOC) such that the less energy stored ($SOC \cong 0$) its threshold increases to prevent it from being activated. Finally, Eq. 22 is the probability that the energy storage agent gives energy (step 4).

$$s_{BAT,S}(t+1) = s_{BAT,S}(t) + w_{BAT,S} Soc (P_L - P_H) \quad (20)$$

$$\begin{aligned} \theta_{BAT,S}(t+1) &= \theta_{BAT,S}(t) - \beta_{BAT,S} Soc \Delta t \\ &+ \gamma_{BAT,S} (1 - Soc) \Delta t \end{aligned} \quad (21)$$

$$q_{BAT,S}(t) = \frac{s_{BAT,S}(t)^2}{s_{BAT,S}(t)^2 + \theta_{BAT,S}(t)^2} \quad (22)$$

Consumer:

Next, we present steps 1 and 2 of the design process in this agent as a consumer:

- Behaviour: It is a consumer when there is a surplus of renewable energy and it does not have enough stored energy.
- Environment: Does not apply
- External variables: Demand and renewable sources.
- Internal variables: SOC.

Steps 3 and 4 define the self-control mechanism and the activation probability based on the RTM of this agent as a consumer. Eq. 23 describes that the consumption state occurs when the batteries are discharged ($Soc \cong 0$) and there is surplus energy from the renewable system. Also, the threshold (Eq. 24) is adjusted when the batteries are discharged ($SOC \cong 0$) such that the less energy stored its threshold decreases to activate it. Finally, Eq. 25 is the probability that the energy storage agent consumes energy (step 4).

$$s_{BAT,C}(t+1) = s_{BAT,C}(t) + w_{BAT,C} (1 - Soc) (P_H - P_L) \quad (23)$$

$$\begin{aligned} \theta_{BAT,C}(t+1) &= \theta_{BAT,C}(t) - \beta_{BAT,C} (1 - Soc) \Delta t \\ &+ \gamma_{BAT,C} (Soc) \Delta t \end{aligned} \quad (24)$$

$$q_{BAT,C}(t) = \frac{s_{BAT,C}(t)^2}{s_{BAT,C}(t)^2 + \theta_{BAT,C}(t)^2} \quad (25)$$

Passive:

$q_{BAT,P}$ is the probability of the passive state based on the previous probabilities.

$$q_{BAT,P}(t) = 1 - (q_{BAT,S}(t) + q_{BAT,C}(t)) \quad (26)$$

4) PROSUMER AGENT

This section presents the RTM applied to the exchange agent or the MG as a prosumer, which is responsible for establishing trade with adjacent MGs. This emergent control system must handle three states, such as buyer (consumer), seller (producer), or passive. The agent monitors the surplus or deficit in the MG to control the exchange of energy, taking into account as surplus the generation of renewable energy sources such as solar (Eq. 4), wind (Eq. 6), geothermal (Eq. 8), etc., and the total consumption of the MG (see Eq. 12). Specifically, ΔP can be redefined as:

$$\Delta P = (P_H + P_{ESS}) - P_L \quad (27)$$

The equations of this emergent control system are:

Producer:

Next, we present steps 1 and 2 of the design process in this agent as a producer:

- Behaviour: This agent will be activated when there is a surplus the generation of renewable energy sources that can sell.
- Environment: Does not apply
- External variables: Local and adjacent MG.
- Internal variables: Does not apply.

Steps 3 and 4 define the self-control mechanism and the activation probability based on the RTM of this agent as a producer. Eq. 28 represents the stimulus that will increase when the surplus of the local MG is greater than the neighboring MG ($(\Delta P_{local} - \Delta P_{neighbor}) > 0$). On the other hand, the threshold decreases when the locally generated power can satisfy the demand of the neighboring MG ($(\frac{\Delta P_{local}}{P_{L,neighbor}} > 0)$) (see Eq. 29). Finally, Eq. 30 is the probability that the MG gives (buys) energy to its neighbors (step 4).

$$s_{LINE,P}(t+1) = s_{LINE,P}(t) + w_{LINE,P} (\Delta P_{local} - \Delta P_{neighbor}) \quad (28)$$

$$\begin{aligned} \theta_{LINE,P}(t+1) &= \theta_{LINE,P}(t) - \beta_{LINE,P} \left(\frac{\Delta P_{local}}{P_{L,neighbor}} \right) \Delta t \\ &+ \gamma_{LINE,P} \left(1 - \frac{\Delta P_{local}}{P_{L,neighbor}} \right) \Delta t \end{aligned} \quad (29)$$

$$q_{LINE,P}(t) = \frac{s_{LINE,P}(t)^2}{s_{LINE,P}(t)^2 + \theta_{LINE,P}(t)^2} \quad (30)$$

Consumer:

Next, we present steps 1 and 2 of the design process in this agent as a consumer:

- Behaviour: This agent will be activated when the MG needs to buy energy (when the solar or wind potential is not enough to satisfy the demand and it has not stored energy).
- Environment: Does not apply
- External variables: Local and adjacent MG.
- Internal variables or parameters: Does not apply.

Steps 3 and 4 define the self-control mechanism and the activation probability based on the RTM of this agent as a consumer. Eq. 31 represents the stimulus that will increase when the surplus of the neighboring MG is greater than the local MG ($(\Delta P_{neighbor} - \Delta P_{local} > 0)$). On the other hand, the threshold is decreased when the power generated by the neighboring MG can satisfy the demand of the local MG ($(\frac{\Delta P_{neighbor}}{P_{L,local}} > 0)$) (see Eq. 32). Finally, Eq. 33 is the probability that the MG consumes (sells) energy from its neighbors (step 4).

$$s_{LINE,P}(t+1) = s_{LINE,P}(t) + w_{LINE,P} (\Delta P_{neighbor} - \Delta P_{local}) \quad (31)$$

$$\begin{aligned} \theta_{LINE,P}(t+1) &= \theta_{LINE,P}(t) - \beta_{LINE,P} \left(\frac{\Delta P_{neighbor}}{P_{L,local}} \right) \Delta t \\ &+ \gamma_{LINE,P} \left(1 - \frac{\Delta P_{neighbor}}{P_{L,local}} \right) \Delta t \end{aligned} \quad (32)$$

$$q_{LINE,C}(t) = \frac{s_{LINE,C}(t)^2}{s_{LINE,C}(t)^2 + \theta_{LINE,C}(t)^2} \quad (33)$$

586 Passive: Eq. 34 represents the probability of the passive
587 state.

$$588 \quad q_{LINE,N}(t) = 1 - (q_{LINE,C}(t) + q_{LINE,p}(t)) \quad (34)$$

589 5) UTILITY GRID AGENT

590 These energy sources, generally from fossil fuels, are used
591 when there are no other options and they must be paid at
592 the market price. In steps 1 and 2 of the design process,
593 we identify and analyse the variables, context, and dynamics
594 of this agent.

- 595 • Behaviour: It is activated when renewable sources do not
596 meet the demand.
- 597 • Environment: Does not apply
- 598 • External variables: Demand and renewable sources.
- 599 • Internal variables or parameters: Does not apply.

600 Steps 3 and 4 define the self-control mechanism and the
601 activation probability based on the RTM of this agent. The
602 RTM applied for the utility grid agent is described in Eq. (35).
603 The agent is stimulated when the demand P_L is greater than
604 the power of renewable sources (P_H), energy storage system
605 (P_{ESS}) and synchronous generators (P_{SG}) such as geothermal
606 plants ($[P_L - (P_H + P_{ESS} + P_{SG})] > 0$). Also, the threshold
607 is decreased when the ratio between power from demand and
608 sources is not sufficient ($\frac{P_L}{P_H + P_{ESS} + P_{SG}} > 0$) (see Eq. (36)).
609 Finally, $q_{UG}(t)$ is the probability of activating or not activating
610 the switch (See Eq. 37) (step 4).

$$611 \quad s_{UG}(t+1) = s_{UG}(t) + w_{UG} [P_L - (P_H + P_{ESS} + P_{SG})] \quad (35)$$

$$612 \quad \theta_{UG}(t+1) = \theta_{UG}(t) - \beta_{UG} \left(\frac{P_L}{P_H + P_{ESS} + P_{SG}} \right) \Delta t$$

$$613 \quad + \gamma_{UG} \left(1 - \frac{P_L}{P_H + P_{ESS} + P_{SG}} \right) \Delta t \quad (36)$$

$$614 \quad q_{UG}(t) = \frac{s_{UG}(t)^2}{s_{UG}(t)^2 + \theta_{UG}(t)^2} \quad (37)$$

615 6) GEOTHERMAL GENERATION AGENT

616 Steps 1 and 2 of the design process for this agent define the
617 next information:

- 618 • Behaviour: This agent will be activated when its stimu-
619 lus tends to increase, which occurs when there is inlet
620 temperature of the primary (geothermal) fluid (T_{in}),
621 demand (P_L), and there is no energy stored in the
622 batteries ($1 - Soc$).
- 623 • Environment: Inlet temperature of the primary (geother-
624 mal) fluid (T_{in})
- 625 • External variables: Demand and status/capacity of the
626 ESS (battery).
- 627 • Internal variables or parameters: Available thermal
628 power (kW).

629 Steps 3 and 4 define the self-control mechanism and the
630 activation probability based on the RTM of this agent. The
631 RTM applied to the GEO agent is described in Eqs. (38-40).

The agent is stimulated according to the available thermal
632 potential (ATP) (Eq. 38). On the other hand, the threshold is
633 the ratio between the real power delivered by the synchronous
634 generator of the geothermal plant and the total load.
635

$$636 \quad s_{GEO}(t+1) = s_{GEO}(t) + w_{GEO} (P_{GEOmax} (P_L$$

$$637 \quad + (1 - Soc) Q_{CAP})) \quad (38)$$

$$638 \quad \theta_{GEO}(t+1) = \theta_{GEO}(t) - \beta_{GEO} \left(\frac{P_{GEO}}{P_L} \right) \Delta t$$

$$639 \quad + \gamma_{GEO} \left(1 - \frac{P_{GEO}}{P_L} \right) \Delta t \quad (39)$$

$$640 \quad q_{GEO}(t) = \frac{s_{GEO}(t)^2}{s_{GEO}(t)^2 + \theta_{GEO}(t)^2} \quad (40)$$

641 V. SIMULATION STUDY

642 In these sections are presented the case studies to be analyzed,
643 the metrics used to evaluate the quality of our proposal,
644 a detailed discussion of the results obtained in each case
645 study, and finally, a general analysis of the results.

646 A. EXPERIMENTAL PROTOCOL

647 To validate our approach, we address some case studies,
648 each with different interesting properties. The experiments
649 recreate different operational scenarios, such as variations
650 in the dynamics of the renewable generation systems due to
651 weather conditions, battery charging/discharging processes,
652 energy trade, the effect of EV uncontrolled load variations,
653 and compensation of the main grid in the event of deficiencies
654 in the other components of the MG. The power units will be
655 expressed in watts [W]. The quality of the results obtained is
656 evaluated using the next performance criteria [36]:

- 657 • Integral square error (ISE): the errors are penalized with
658 large values. A control error normally occurs after a
659 disturbance and can be observed as an overshoot. Thus,
660 this index indicates overshoot and aggressive control.

$$661 \quad ISE = \int_{t_1}^{t_2} \varepsilon(t)^2 dt \quad (41)$$

- 662 • Integral Absolute Error (IAE): it does not distinguish
663 between positive and negative contributions to the error.
664 It is often used for on-line controller tuning. This index
665 is appropriate for non-monotonic step responses and all
666 kinds of normal operations (see Eq. (42)).

$$667 \quad IAE = \int_{t_1}^{t_2} |\varepsilon(t)| dt \quad (42)$$

- 668 • Mean relative absolute error (MrAE): This index of error
669 is useful in order to show the correlation between the
670 bias of a model and a parameter that can be an input or
671 another variable (see Eq. (43)) [37].

$$672 \quad MrAE = \frac{1}{N} \sum_i^N \frac{|x_{model,i}(t) - x_{meas,i}(t)|}{x_{meas}(t)} \quad (43)$$

673 On the other hand, an objective function J is used
674 to determine the optimal hyperparameters of our model

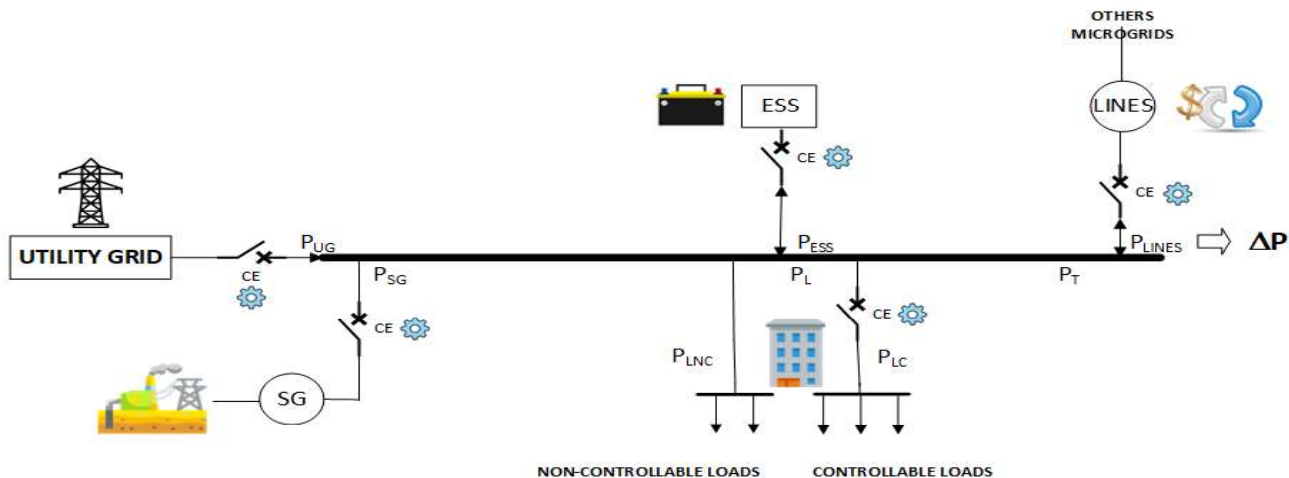


FIGURE 2. Scenery of a slack MG.

TABLE 1. Parameter values used in the simulation of each component of the model.

Parameter	Symbol	PV	Wind Turbine	Battery producer	Battery consumer	Exchange agent	Utility grid	Geothermal generation
Initial stimulus s_i	s	100	100	100	100	100	100	100
Initial response threshold θ_{ij}	θ	100	100	100	100	100	100	100
Attenuation factor	W	10.1×10^{-6}	5.00×10^{-6}	5.00×10^{-6}	5.00×10^{-6}	5.00×10^{-8}	5.00×10^{-8}	10.10×10^{-6}
Learning factor	β	1.06×10^{-6}	1.00×10^{-6}	1.00×10^{-6}	1.00×10^{-6}	1.00×10^{-6}	1.00×10^{-6}	1.06×10^{-6}
Forgetting factor	γ	3.00×10^{-5}	1.00×10^{-6}	1.00×10^{-6}	1.00×10^{-6}	3.90×10^{-5}	3.90×10^{-5}	3.00×10^{-5}

(see Eq. (44)), in order to achieve an error close to zero. Particularly, it was used the search grid algorithm to adjust the parameters of our model.

$$J_i = \min\{ISE(\Delta P)\} \tag{44}$$

Thus, the metrics presented above are used to determine the quality of our approach in the case studies, due to the absence of similar works. Also, they are used during the tuning process of our model (the optimization of its hyperparameters) in each case study. The calibration procedure allows the estimation of the values for β and γ (the adjustment is made), in such a way that the objective function of Eq. 44 is minimized.

B. TESTS AND DISCUSSIONS

In this section, some case studies are presented, in order to show the versatility of our approach. Table 1 summarizes the parameters obtained from the hyperparameters optimization process.

1) CASE STUDY 1: HIGH ATP (AVAILABLE GEOTHERMAL POTENTIAL)

In this case study, presented in Fig. 2, the scenario of a MG whose main characteristic is the capacity for interconnection

to the public grid and synchronous generators (GEO agent) will be analyzed, with components as an ESS, and a connection line with other MGs. Each of these components has a discrete control agent, which allows them to be coordinated to meet the demand of the MG and the load of the ESS. In addition, the purchase/sale of energy to its neighboring MGs is prioritized before the main energy network due to cost differences. In this case, the control of normal loads will not be considered, it will only be assumed that the total demand of the MG must be satisfied through the available energy sources. For this, the geothermal potential is high, with sufficient capacity to supply the local load and sell to its neighboring's, and there is no contribution from wind or solar sources. The tests will be carried out in a period of 20 continuous days.

In Fig. 3 can initially be observed (time 0) that the geothermal generation is high (see Fig. 3.A) and with enough capacity to satisfy the demand (see Fig. 3.E, is 600 MW), so the ESS agent does not come into operation (see Fig. 3.B). When the power is negative, it means that it is sending or transferring the energy of the current MG to another, motivated by the fact that the exchange agent detected excess in the current MG and deficit in the neighboring MG. On the other hand, the UG agent does not come into operation (see Fig. 3.D) because

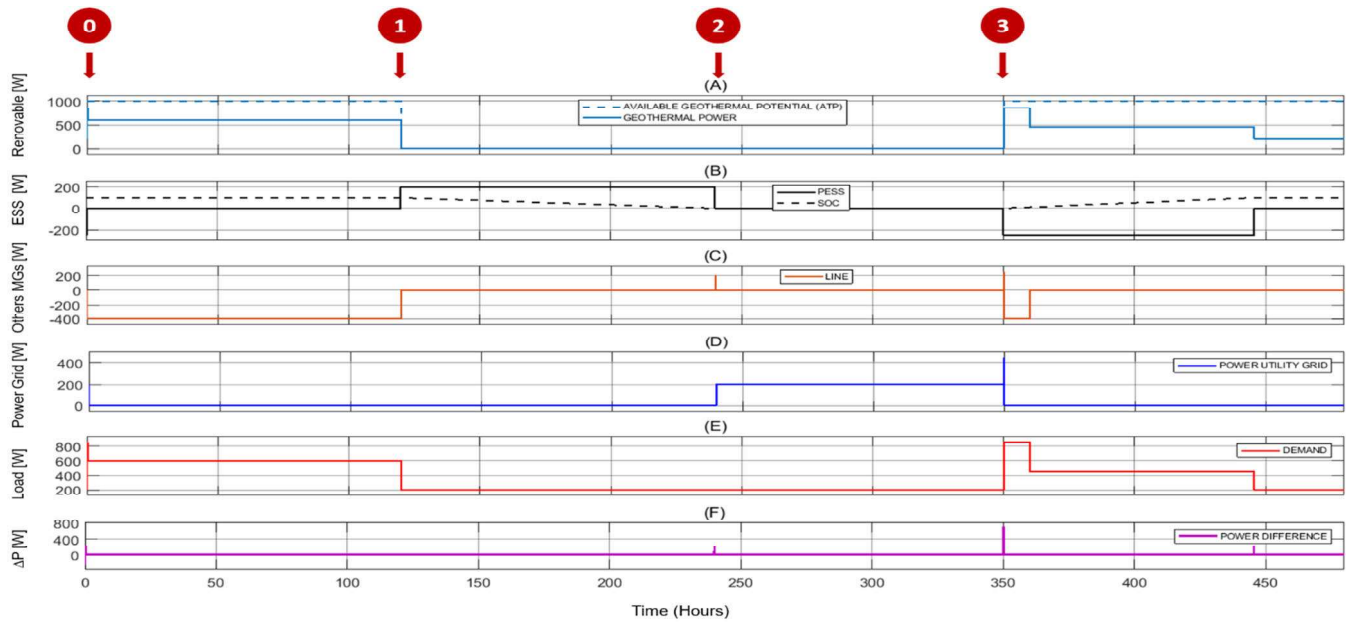


FIGURE 3. Scenery of slack MG. A) Dotted lines represent the geothermal generation potential and continuous lines the real power delivered. B) The dotted lines show the percentage of battery charge and the continuous lines show the real power delivered by the ESS. C) Power difference with neighbouring MG. D) Power supplied from the UG agent E) Demand or load. F) Difference between the total input and consumed energy.

720 the generation of the GEO agent is enough. At the time 1,
 721 a fault occurs in the GEO agent (geothermal power plant, see
 722 Fig. 3.A), which forces the supply to be compensated with the
 723 activation of the ESS, which is supposed to be loaded (see
 724 Fig. 3.B) and can satisfy the local MG. It should be noted
 725 that the behavior of interest is the dotted line represented
 726 by SOC in Fig. 3.B, which means the percentage of battery
 727 charge, while the continuous line shows positive values when
 728 it produces and negative values when it consumes.

729 At time 2, the fault in the GEO agent persists (see Fig. 3.A),
 730 the ESS is discharged (see Fig. 3.B) and there is no demand
 731 for energy with the neighboring MG (see Fig. 3.C), so the
 732 UG agent comes into operation (see Fig. 3.D), satisfying the
 733 local demand (see Fig. 3.E) and guaranteeing the balance of
 734 energy in the MG (see Fig. 3.F). Thus, when the EES agent
 735 load decreases (time 2), then the demand is covered by the UG
 736 agent. At time 3, the GEO agent is restored (see Fig. 3.A),
 737 so the supply of the UG agent is interrupted (see Fig. 3.D),
 738 and the local demand is satisfied (see Fig. 3.E). Thus, when
 739 the GEO agent is reactivated (time 3), then the MG load is
 740 covered. An important aspect to highlight is that the demand
 741 of the neighboring MG cannot be satisfied (see the interval
 742 between times 0 and 1, and time 3 in Fig 3.C).

743 Finally, Fig. 4.F shows that the balance of supply and
 744 consumption is around 0, reflected in the IAE of 62.13, which
 745 is a very low value for the period of study. On the other hand,
 746 the ISE of 2.53×10^4 is high due to the peaks that occur
 747 in the transitions to achieve the coordination actions of the
 748 MG agents, in order to work together and in a distributed
 749 way to satisfy the MG demand no matter if failures occur or
 750 not (failure/restoration of the GEO agent), or discharge of the
 751 ESS agent.

752 2) CASE STUDY 2: SELF-SUSTAINING BUILDING AS A 753 PROSUMER

754 In this case, a self-sustaining building is analyzed, which has
 755 an array of solar panels on the roof, capable of supplying the
 756 entire building when conditions are favorable (see Fig. 4).
 757 Also, the MG has an ESS, an interconnection equipment to
 758 the neighboring MG but without connection to the utility grid,
 759 such that it has to buy or sell when necessary. On the other
 760 hand, a study period of 20 days is established with favorable
 761 weather conditions with clear skies.

762 Time 0 is mainly characterized by the deficit in the neigh-
 763 bouring MG, expressed by the negative magnitude of the
 764 brown dotted line (see Fig. 5.D). Also, the producers are the
 765 solar panels during the day (see Fig. 5.A) and the ESS during
 766 the night (see Fig. 5.B), in alternation to the solar cycle.
 767 In addition, the ESS is fully charged (see Fig. 5.C) thanks
 768 to the surplus of solar energy. On the other hand, energy is
 769 transferred to the neighboring MG, visualized in the nega-
 770 tive values of the continuous blue line, which is maintained
 771 during excess solar energy (see Fig. 5.D), guaranteeing a
 772 stable and safe supply during the first 10 days, reflected in
 773 the demand, which satisfies both the local and remote loads
 774 (see Fig. 5.E and 5.D).

775 From time 1, which is characterized by a decrease in
 776 demand (see Fig. 5.E) and the excess in the neighbouring
 777 MG, is evident a compensation behaviour in the transitions
 778 reflected in the positive peaks (see Fig. 5.D) to purchase
 779 energy from the neighboring MG to satisfy the local's deficit
 780 during the nights to try to load the EES agent.

781 Finally, it is observed the differences between production
 782 and consumption (see Fig. 5.F) with a greater number and
 783 intensity of peaks reflected in an IAE of 4094 and ISE of

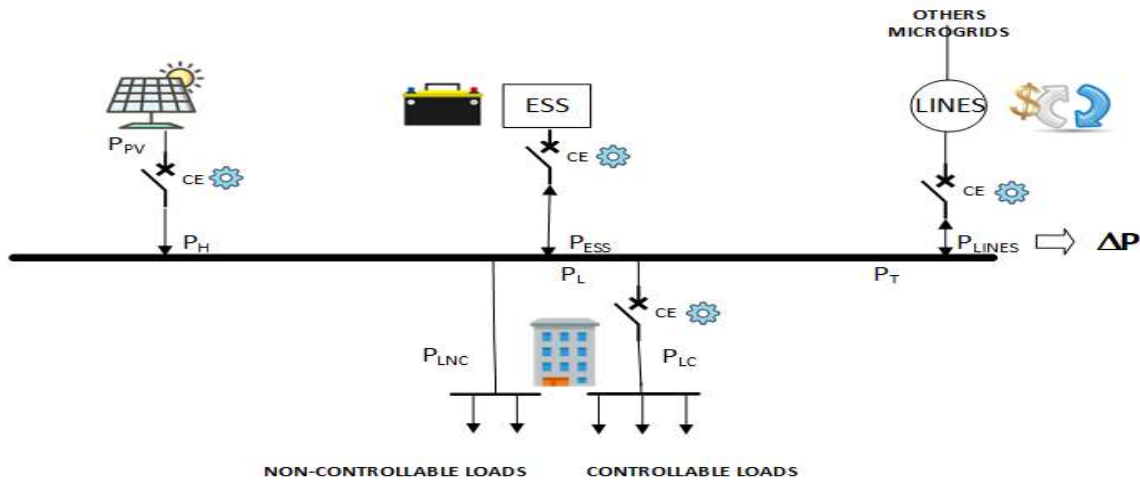


FIGURE 4. Scenery of Self-sustaining building.

784 1.03×10^6 , motivated by the increase in exchanges or transi- 818
 785 tions between the components such as PV, ESS and exchange 819
 786 agents. However, the coordinated work allows maintaining 820
 787 the satisfaction of the demand. 821

788 3) CASE STUDY 3: ELECTRIC VEHICLE (EV) LIKE PROSUMER 822
 789 In the case study of Fig. 6, the main components of an EV 823
 790 ecosystem are analyzed, such as the panels installed in the 824
 791 vehicle body, an ESS, the loads represented by the engine, and 825
 792 connection ports to the charging stations (exchange agent). 826
 793 For this case, randomness in the load is considered in order 827
 794 to emulate the connection or disconnection of the EV to 828
 795 the charging station. In addition, the days are clear, so the 829
 796 maximum use of solar energy is guaranteed in a period of 830
 797 12 days, and the role of the charging station is changed in the 831
 798 last days of the study. 832

799 At time 0, the demand is covered by the generation systems 833
 800 such as the solar panel and the ESS, to continuously supply, 834
 801 depending on the time of day. However, the ESS agent tends 835
 802 to be completely discharged due to random changes in the 836
 803 load in the vehicle (see Fig. 7.E). On the other hand, when 837
 804 the discharge battery is completed at time 1, power must 838
 805 be purchased or consumed from charging stations to meet 839
 806 demand (see Fig. 7.D). 840

807 Finally, the differences between production and consump- 841
 808 tion are observed (see Fig. 7.F) with a higher frequency and 842
 809 intensity of peaks reflected through an IAE of 1.05×10^4 and 843
 810 an ISE of 7.12×10^6 , motivated by the behavior observed 844
 811 from the time 0 to 1, when the PV, ESS and prosumer agents 845
 812 are coordinated (possible energy sale because the solar gener- 846
 813 ation potential is sufficient); while, after time 1, it decreases 847
 814 in intensity since the batteries are discharged. 848

815 4) CASE STUDY 4: WIND POWER IN A MG 849

816 In this case study, the incorporation of a renewable energy 850
 817 component based on the WT agent is analysed (see Fig. 8). 851

818 The MG is made up of ESS, wind generators where random- 819
 820 ness is introduced in the speed, loads without the possibility 820
 821 of control and energy exchange with a neighbouring MG (see 821
 822 Fig. 9). Thus, it is possible to sell or buy the excess energy, 822
 823 when necessary, based on the premise that it is cheaper to 823
 824 buy the available neighbouring energy, instead of the energy 824
 825 coming from the UG agent. The study is carried out over a 825
 826 time period of 12 days. 826

827 Wind speed is a highly random weather variable, so energy 827
 828 production is conditioned by this factor. In Fig. 9.A, the 828
 829 dotted lines represent the wind generation potential and the 829
 830 continuous lines the actual potential delivered. In time 0, 830
 831 the energy only comes from the wind and the participation 831
 832 of the ESS is not necessary (see Fig. 9.B) nor the purchase 832
 833 of energy from neighboring MGs (see Fig. 9.D). In time 1, 833
 834 the wind speed decreases significantly, so the ESS comes into 834
 835 operation, discharging the battery to approximately 75%, due 835
 836 to the increase in load. In time 2, the wind speed remains 836
 837 constant but the load is reduced, which favors a surplus 837
 838 of energy that is used to charge the batteries. However, 838
 839 it is not enough to cover the demand and the charge of the 839
 840 battery, so the purchase of energy from the neighbouring 840
 841 MG is activated, gradually disabling due to the increase in 841
 842 wind generation, reducing again to reactivate the purchase of 842
 843 energy. 843

844 In times 3 and 6, the load is increased and the wind energy 844
 845 is reduced, which results in the activation of the ESS while 845
 846 the wind speed improves. When that happens, the ESS agent 846
 847 is deactivated, changing its role to a consumer, loading again. 847
 848 In times 4 and 7, an emergent behaviour occurs, when the pur- 848
 849 chase of energy is activated instead of activating the batteries 849
 850 that are almost loaded, which is presumed to occur due to the 850
 851 high demand and the low wind generation. In time 5, there 851
 852 is evidence of an increase in wind generation sources relative 852
 853 to the load, which deactivates the batteries and satisfies the 853
 854 demand using only renewable sources. 854

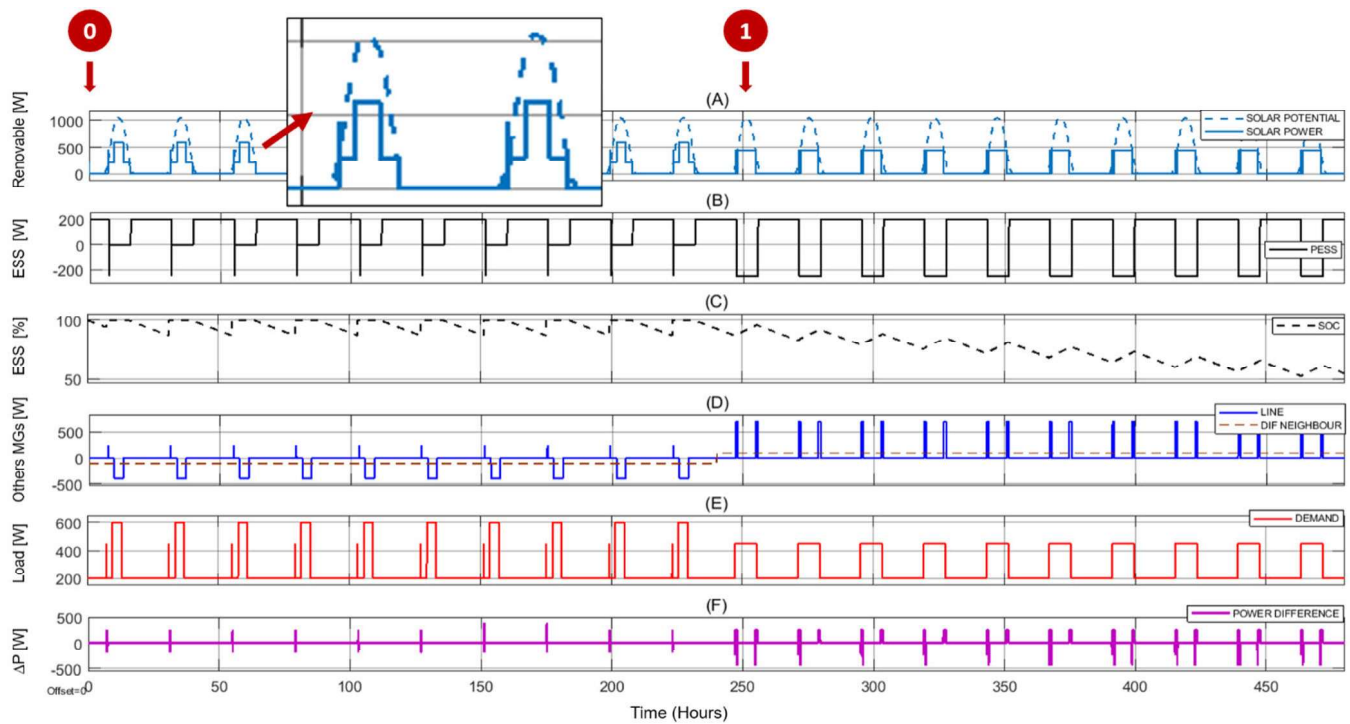


FIGURE 5. Self-sustaining building as a prosumer. A) The dotted lines represent the solar energy potential based on radiation and the continuous lines the real power delivered. B) Power of the ESS, which is positive when it produces and negative when it consumes. C) SOC battery charge percentage. D) The brown dotted lines represent the deficit or excess in the neighboring bus, that is, when it is negative then it is a deficit, and it is positive when it is excess, and the continuous blue line is the power exchanged between the MGs E) Bus demand. F) Difference between total production and consumption.

854 Finally, it is observed in the difference between production
 855 and consumption that there is a big number and intensi-
 856 tity of peaks reflected in an IAE of 3747 and ISE of
 857 5.69×10^5 , motivated by the increase in exchanges or transi-
 858 tions between the various components. However, the coordi-
 859 nated work manages the satisfaction of the demand.

860 5) CASE STUDY 5: SELF-SUSTAINING BUILDING WITH REAL
 861 DATASETS

862 This case study is based on the work of Alam et al. [41],
 863 for which uses its datasets of profiles of solar power, and
 864 consumption, among others, for a year, divided into average
 865 values per week grouped into 4 climatic periods according to
 866 the Hindu calendar seasons. Thus, summer is a hot climate
 867 from week 1 to 13, monsoon is characterized by abundant
 868 rains from week 14 to 26, autumn is a warm and humid
 869 period from week 27 to 35, and winter is a period where
 870 low temperatures predominate from week 36 to 52. However,
 871 for the purposes of our work, we are not considering the
 872 entire year but 2 adjacent weeks for each climatic period.
 873 Specifically, weeks 6 and 7 for summer, weeks 20 and 21 for
 874 monsoon, weeks 32 and 33 for autumn, and weeks 44 and
 875 45 for winter. In this way, the generation and consumption
 876 profiles were used in our simulations for these weeks, which
 877 will allow a fairly approximate scenario according to the
 878 climatic season.

879 In this case study, an isolated self-sustaining building is
 880 analyzed, composed of an array of solar panels on the roof,

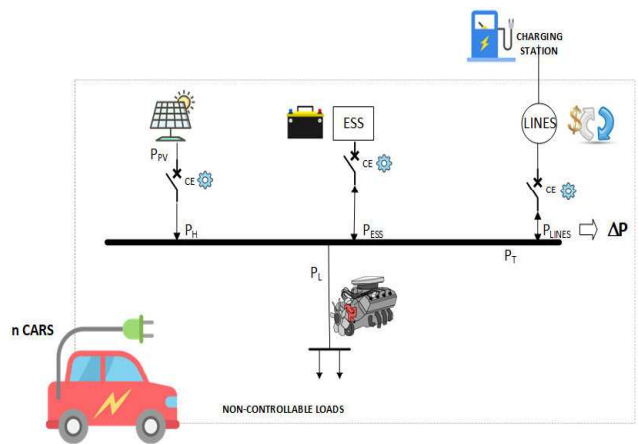


FIGURE 6. Scenery of EVs as a prosumer.

881 capable of supplying the entire building when conditions are
 882 favorable, and an ESS in the building as a backup but without
 883 connection to the public network (see Figure 10).

884 In summer, it is where solar radiation is best used due
 885 to its intensity and duration, observing in figure 11.A that
 886 the solar panels satisfy the demand and recharge the bat-
 887 teries (see figure 11.B / 11.C), evidencing a peak due to
 888 the transitions of the PV/ESS (Figure. 11.E). In monsoon
 889 and autumn, the capacity of the solar panels is significantly
 890 reduced (Figure 11.A), forcing the ESS to meet the demand,

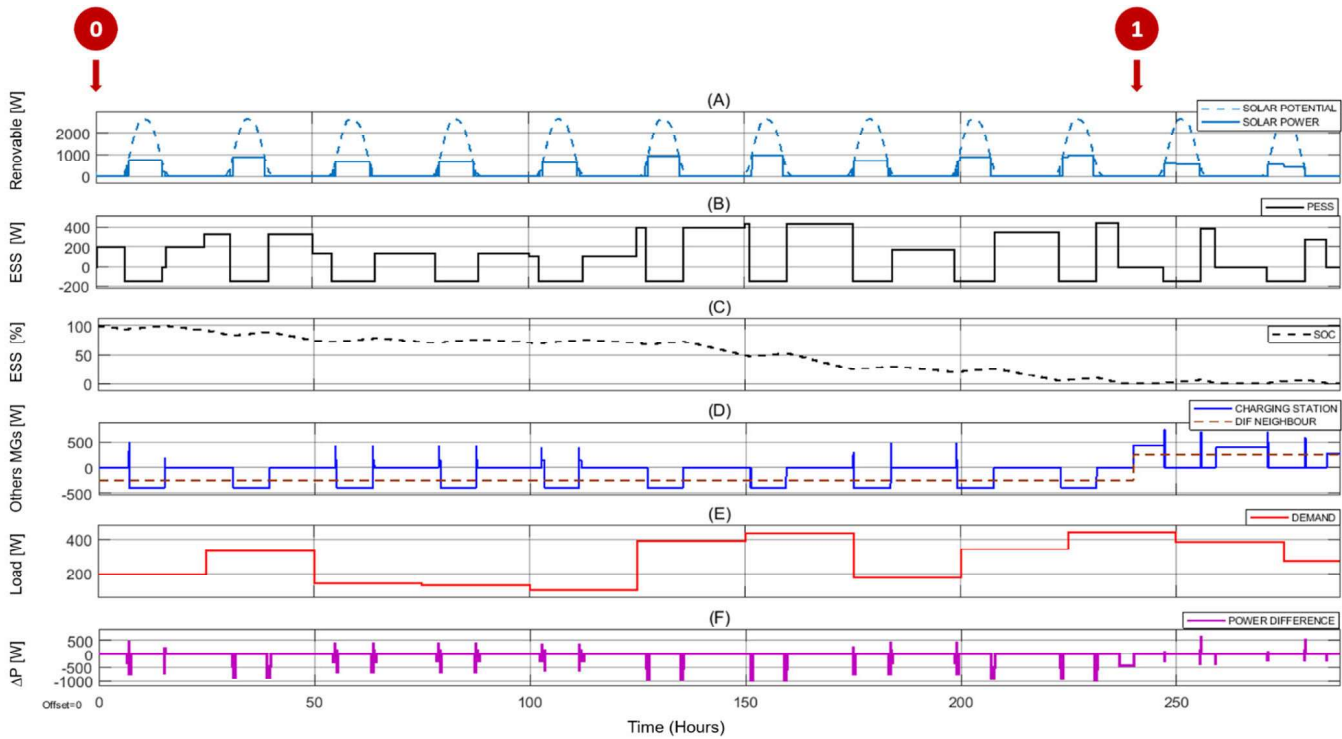


FIGURE 7. EV as a prosumer. A) The dotted lines represent the solar energy potential based on radiation and the continuous lines the real power delivered. B) Power of the ESS, positive when it produces and negative when it consumes. C) SOC battery charge percentage. D) The brown dotted lines represent the deficit or excess in the neighboring MG, that is, when it is negative then it is deficit and positive when it is excess, and the continuous blue line is the power in the charging station E) EV demand. F) Difference between total production and consumption.

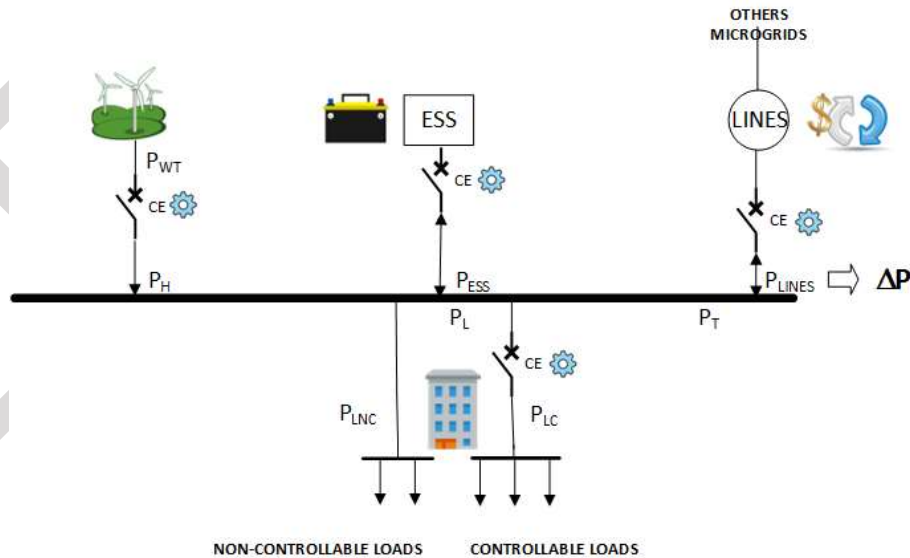


FIGURE 8. Scenery of a wind power in a MG.

891 which causes it to discharge more quickly (Figure 11.C).
 892 This shows that this isolated topology is neither viable nor
 893 recommended for more than half the year, as it limits the
 894 recharging capacity of the batteries from renewable energy
 895 sources. Finally, in winter, solar radiation increases but not
 896 its duration, and the batteries have little time to charge again.

897 Finally, the differences between production and consumption
 898 are observed (see Fig. 11.F) with a greater number and
 899 intensity of peaks in spring and winter, reflected in an IAE
 900 of 3840 and ISE of 3.63×10^6 , motivated by the increase in
 901 exchanges or transitions between components such as PV and
 902 ESS when radiation allows demand to be met.

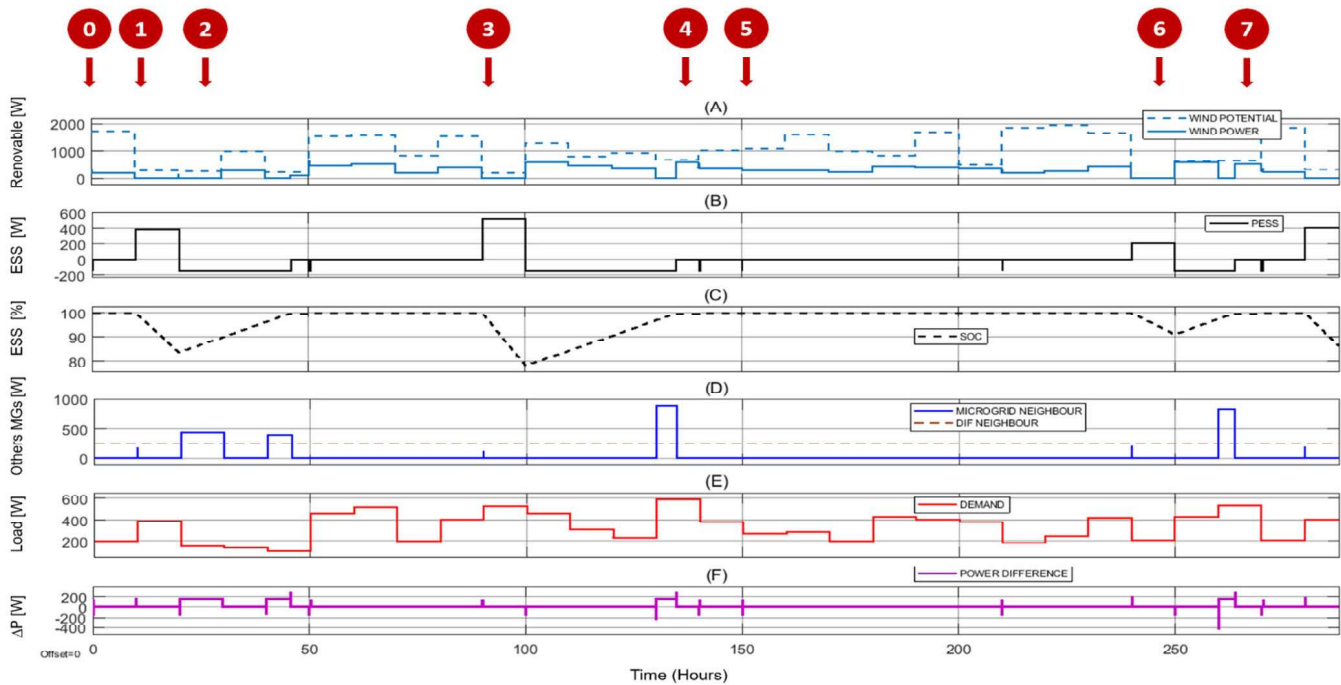


FIGURE 9. Wind power in a MG. A) The dotted lines represent the wind energy potential and the continuous lines the real power delivered. B) Power of the ESS. C) SOC battery charge percentage. D) The brown dotted lines represent the excess in the neighboring MG and the continuous blue line is the power exchanged between the MGs E) Bus demand. F) Difference between total production and consumption.

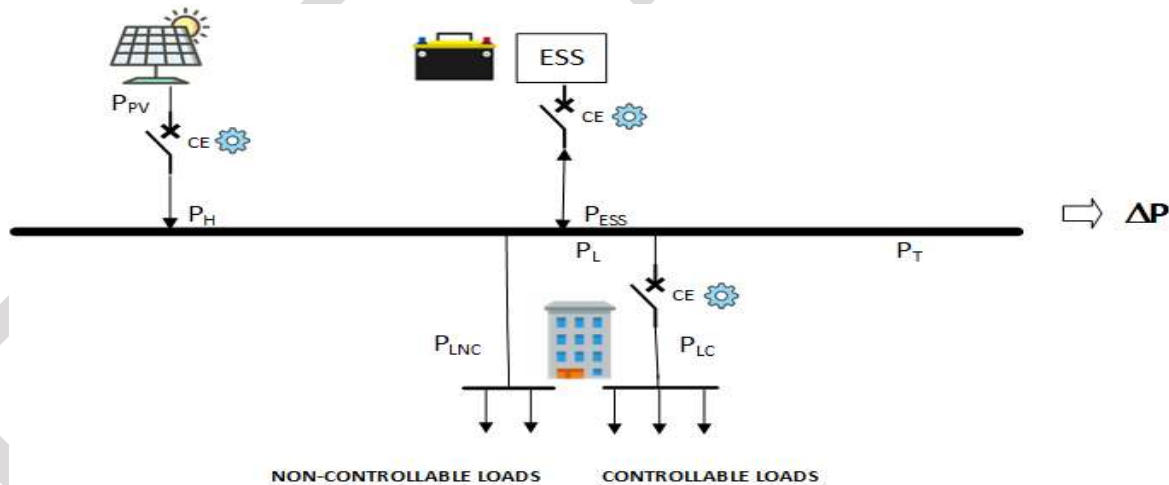


FIGURE 10. Scenery of Self-sustaining building with real datasets.

6) CASE STUDY 6: WIND POWER IN A MG WITH REAL DATASETS

In this case study are used the same datasets from work [41], used in the previous case study. This case study considers an isolated self-sustaining building made up of a group of turbines, capable of supplying the entire building when conditions are favorable, and an ESS as a backup but without connection to the public network (see Fig. 12).

It is observed that in summer and winter, the wind speed is significant to satisfy the demand, but the same does not happen in monsoon and autumn (Figure 13.A), where the ESS

plays a fundamental role to cover the energy needs of customers in the absence of wind energy (Figure 13.B and 13.C), causing them to discharge considerably. Thus, it is not a recommended topology for half the year. The peaks observed in figure 13.E are the result of the transitions between the generation sources. Finally, it is observed in the difference between production and consumption that there is a big number and intensity of peaks reflected in an IAE of 1388 and ISE of 5.7×10^5 , motivated by the increase in exchanges or transitions between the various components.

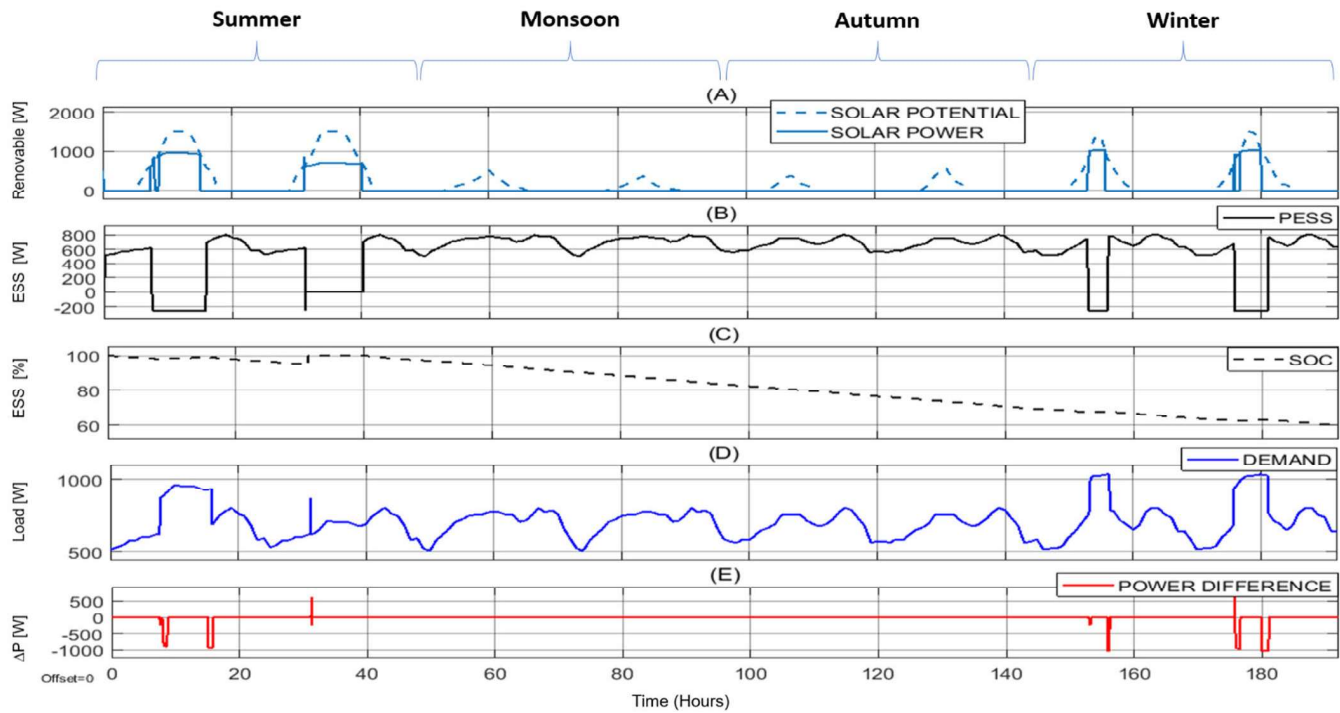


FIGURE 11. Self-sustaining building. A) The dotted lines represent the solar energy potential based on radiation and the continuous lines the real power delivered. B) Power of the ESS, which is positive when it produces and negative when it consumes. C) SOC battery charge percentage. D) Bus demand. E) Difference between total production and consumption.

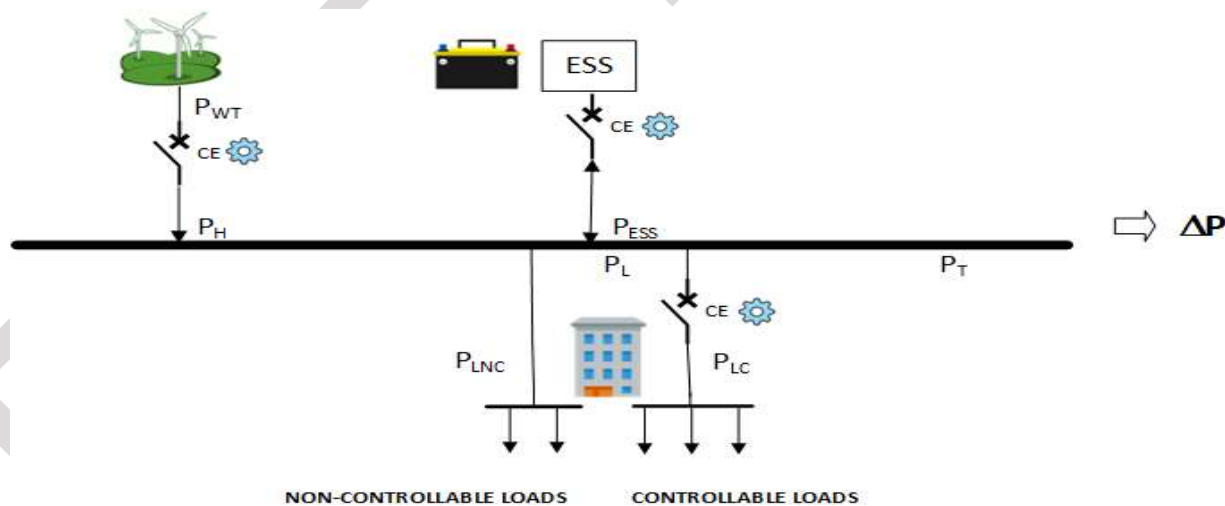


FIGURE 12. Scenery of a wind power in a MG with real datasets.

925 These last scenarios highlight the importance of inter-
 926 connected MGs communities to give greater robustness and
 927 resilience to electrical networks.

928 **C. DISCUSSION OF THE RESULTS**

929 Table 2 summarizes the results obtained from the previous
 930 case studies. IAE measures the error over time and IAE the
 931 peaks in magnitude and frequency, which expresses the transi-
 932 tions in the different components or with other MGs. Each
 933 case study explores situations that can occur in an energy
 934 network such as variability of climatic conditions (e.g., the

wind speed), component failures (e.g., in the GEO agent),
 935 changes in consumer demand, exchanges of energy with a
 936 neighboring MG, randomness in the consumption of EVs,
 937 among others.
 938

939 When observing the MrAE metric, it is evident that most
 940 of the time, the 6 cases were close to the real value, which
 941 in this case refers to the demand, where the peaks caused the
 942 differences in most cases.

943 When analyzing the values obtained, we can conclude
 944 that in all the case studies transitions occur according to the
 945 environmental conditions, and demand change, among other

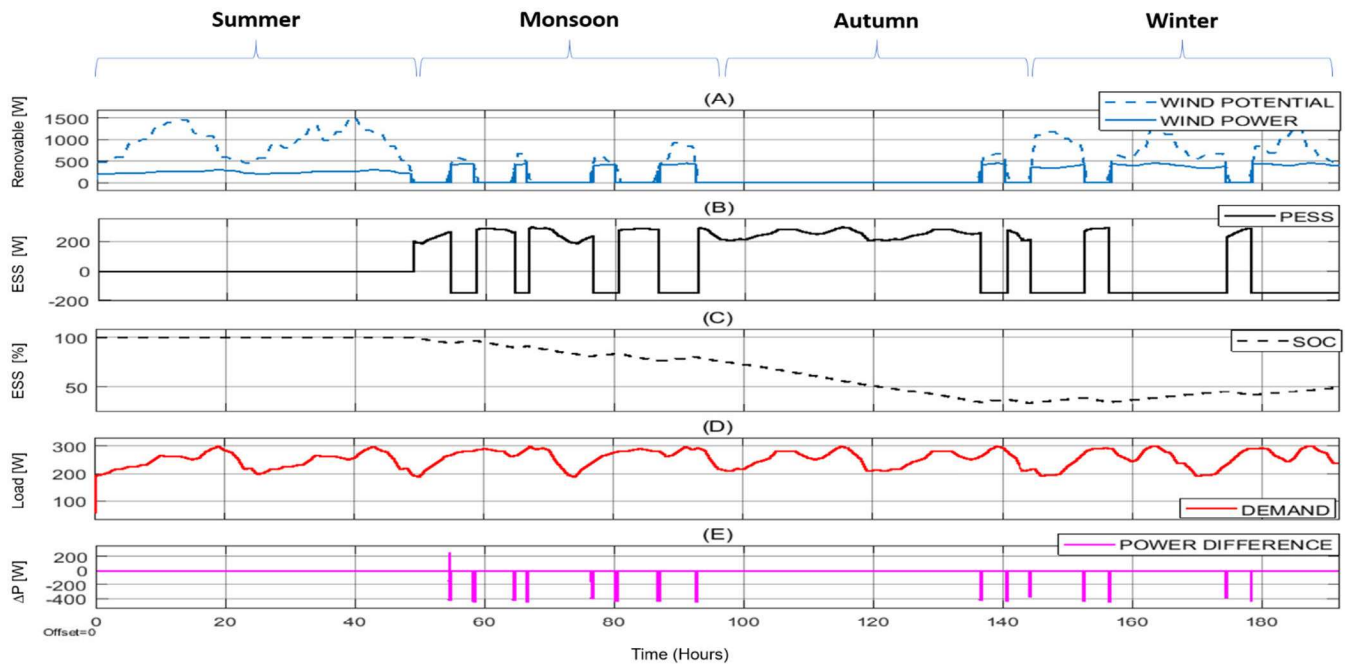


FIGURE 13. Wind power in a MG. A) The dotted lines represent the wind energy potential and the continuous lines the real power delivered. B) Power of the ESS. C) SOC battery charge percentage. D) Bus demand. E) Difference between total production and consumption.

TABLE 2. Summary of metrics of the case studies.

	Case 1	Case 2	Case 3	Case 4	Case 5	Case 6
IAE	62.13	4094	1.05×10^4	3747	3840	1388
ISE	2.53×10^4	1.03×10^6	7.12×10^6	5.69×10^5	3.63×10^6	5.7×10^5
MrAE	6.47×10^{-4}	4.26×10^{-2}	3.36×10^{-1}	3.16×10^{-2}	3.13×10^{-2}	0.0301

AQ:7

946 reasons, which generates changes in the magnitude and fre-
 947 quency of peaks. The minimum occurs when the generation
 948 source is the GEO agent, and the maximum is due to EV
 949 agent, which indicates that the main source of production
 950 influences the stability of the network. Sources such as wind
 951 and solar energy have relatively similar values, showing a
 952 lower degree in the WT agent due to its availability at any time
 953 (day and night), unlike solar energy, which is only available
 954 during the day. In general, our bioinspired emergent control
 955 system allows perfect coordination in the different case stud-
 956 ies, always covering the demand using different strategies
 957 depending on the context.

958 **VI. CONCLUSION**

959 This study proposes a bioinspired emergent control archi-
 960 tecture based on RTM. In our work, a MG composed of a
 961 set of heterogeneous agents is perfectly coordinated by our
 962 strategy, in order to meet consumer demand. It is highlighted
 963 the diversity and quantity of components that exist both on the
 964 supply side and on the demand side, increasing the robustness
 965 of the system.

The most important characteristic of our approach is its
 966 robustness, given that, in the event of failure of any of the
 967 components, or changes in the climatic conditions, or changes
 968 in demand, the agents adapt to respond to unforeseen condi-
 969 tions, and thus guarantee the achievement of global objec-
 970 tives (the demand). Another contribution of the work was
 971 the incorporation of exchange agents to control the flow of
 972 energy between neighbouring MGs (sell/purchase of energy).
 973 The results obtained show its potential to solve some of the
 974 challenges around the energy ecosystems that currently exist:
 975 i) Local marketing of energy surpluses; ii) managing of the
 976 unpredictability of EVs; iii) distributed coordination based
 977 only on local information of the environment; iv) very fast
 978 transitions, v) prioritization of renewable supply sources.

979 From the results obtained, it can be concluded that the
 980 bioinspired emergent control approach can be adapted to var-
 981 ious contexts, to achieve coordinated and distributed control
 982 actions between components. In addition, it is evident that
 983 the main source of production influences the stability of the
 984 network. The work developed is limited solely to studying the
 985 power contributions between the various agents of the energy
 986 ecosystem, which were modeled in a simple way, without
 987 taking into account the electrical complexities of each one
 988 such as voltage control, and converters, among others.

989 In future works, it is proposed to deepen the control on
 990 the demand side, through the scheduling of the controllable
 991 loads, detailing the equipment contained in a house or apart-
 992 ment by the specification and prioritization of appliances,
 993 considering the energy costs in the market, the life patterns
 994 of the users, etc. It is also proposed to explore other emerging
 995

control models such as deep dynamic reinforcement learning, among others. Although the focus of future work revolves around the problem of distributed control, it could delve into other more complex models of the components, as well as apply MG design methodologies to size the components according to various needs or operational requirements. Finally, future works should study the different business relationships between MG communities, as some may be collaborative, others require negotiation mechanisms, etc.

DISCLAIMER

The content of this publication does not reflect the official opinion of the European Union. Responsibility for the information and views expressed herein lies entirely with the author(s).

REFERENCES

- [1] X. Li, D. Zhang, T. Zhang, Q. Ji, and B. Lucey, "Awareness, energy consumption and pro-environmental choices of Chinese households," *J. Cleaner Prod.*, vol. 279, Jan. 2021, Art. no. 123734.
- [2] H. Lo, S. Blumsack, P. Hines, and S. Meyn, "Electricity rates for the zero marginal cost grid," *Electr. J.*, vol. 32, no. 3, pp. 39–43, Apr. 2019.
- [3] E. Sarker, P. Halder, M. Seyedmahmoudian, E. Jamei, B. Horan, S. Mekhilef, and A. Stojcevski, "Progress on the demand side management in smart grid and optimization approaches," *Int. J. Energy Res.*, vol. 45, no. 1, pp. 36–64, 2021.
- [4] Y. H. Lin and Y. C. Hu, "Residential consumer-centric demand-side management based on energy disaggregation-piloting constrained swarm intelligence: Towards edge computing," *Sensors*, vol. 18, no. 5, pp. 1–13, 2018.
- [5] K. Kotilainen, "Energy prosumers' role in the sustainable energy system," in *Affordable and Clean Energy. Encyclopedia of the UN Sustainable Development Goals*, Cham, Switzerland: Springer, 2021, pp. 507–520.
- [6] T. R. Bajracharya, S. R. Shakya, and A. Sharma, "Energy and environment: Sustainability and security," in *Handbook of Energy and Environmental Security*, Jan. 2022, pp. 469–480.
- [7] P. Ray, S. Mohanty, and N. Kishor, "Small-signal analysis of autonomous hybrid distributed generation systems in presence of ultracapacitor and tie-line operation," *J. Electr. Eng.*, vol. 61, no. 4, pp. 205–214, Jul. 2010.
- [8] S. M. Moghaddas-Tafreshi, M. Jafari, S. Mohseni, and S. Kelly, "Optimal operation of an energy hub considering the uncertainty associated with the power consumption of plug-in hybrid electric vehicles using information gap decision theory," *Int. J. Electr. Power Energy Syst.*, vol. 112, pp. 92–108, Apr. 2019.
- [9] N. Nikmehr and S. N. Ravadanegh, "Optimal power dispatch of multi-microgrids at future smart distribution grids," *IEEE Trans. Smart Grid*, vol. 6, no. 4, pp. 1648–1657, Jul. 2015.
- [10] F. Bandejas, E. Pinheiro, M. Gomes, P. Coelho, and J. Fernandes, "Review of the cooperation and operation of microgrid clusters," *Renew. Sustain. Energy Rev.*, vol. 133, Nov. 2020, Art. no. 110311.
- [11] S. Yassine, E. K. Najib, and L. Fatima, "A survey: Centralized, decentralized, and distributed control scheme in smart grid systems," in *Proc. 7th Medit. Congr. Telecommun. (CMT)*, Oct. 2019, pp. 1–11, 2019.
- [12] A. Abhishek, A. Ranjan, S. Devassy, B. K. Verma, S. K. Ram, and A. K. Dhakar, "Review of hierarchical control strategies for DC microgrid," *IET Renew. Power Gener.*, vol. 14, no. 10, pp. 1631–1640, 2020.
- [13] L. Ahmmedzic and M. Music, "Comprehensive review of trends in microgrid control," *Renew. Energy Focus*, vol. 38, pp. 84–96, Sep. 2021.
- [14] S. Sen and V. Kumar, "Microgrid control: A comprehensive survey," *Annu. Rev. Control*, vol. 45, pp. 118–151, Jan. 2018.
- [15] J. Aguilar, J. Giraldo, M. Zapata, A. Jaramillo, L. Zuluaga, and M. D. R.-Moreno, "Autonomous cycle of data analysis tasks for scheduling the use of controllable load appliances using renewable energy," in *Proc. Int. Conf. Comput. Sci. Comput. Intell. (CSCI)*, Dec. 2021, pp. 1862–1867.
- [16] P. Palensky and D. Dietrich, "Demand side management: Demand response, intelligent energy systems, and smart loads," *IEEE Trans. Ind. Informat.*, vol. 7, no. 3, pp. 381–388, Aug. 2011.
- [17] H. J. Touma, M. Mansor, M. S. A. Rahman, V. Kumaran, H. B. Mokhlis, Y. J. Ying, and M. A. Hannan, "Energy management system of microgrid: Control schemes, pricing techniques, and future horizons," *Int. J. Energy Res.*, vol. 45, no. 9, pp. 12728–12739, Jul. 2021.
- [18] A. Abou El-Ela, D. Gado, T. Fetouh, A. Mansour, and S. Moussa, "Power flow management and control of energy storage system for electric vehicles in smart grids," *ERJ. Eng. Res. J.*, vol. 44, no. 3, pp. 263–271, Jul. 2021.
- [19] D. Mathur, N. Kanwar, and S. K. Goyal, "Impact of electric vehicles on community microgrid," in *Proc. AIP Conf.*, vol. 2294, Dec. 2020, Art. no. 040010.
- [20] J. Aguilar, A. Garces-Jimenez, M. D. R.-Moreno, and R. García, "A systematic literature review on the use of artificial intelligence in energy self-management in smart buildings," *Renew. Sustain. Energy Rev.*, vol. 151, Nov. 2021, Art. no. 111530.
- [21] J. Aguilar, O. Buendia, A. Pinto, and J. Gutiérrez, "Social learning analytics for determining learning styles in a smart classroom," *Interact. Learn. Environments*, vol. 30, no. 2, pp. 245–261, Feb. 2022.
- [22] J. Aguilar, C. Salazar, H. Velasco, J. Monsalve-Pulido, and E. Montoya, "Comparison and evaluation of different methods for the feature extraction from educational contents," *Computation*, vol. 8, no. 2, p. 30, Apr. 2020.
- [23] J. Teran, J. Aguilar, and M. Cerrada, "Integration in industrial automation based on multi-agent systems using cultural algorithms for optimizing the coordination mechanisms," *Comput. Ind.*, vol. 91, pp. 11–23, Oct. 2017.
- [24] E. Bonabeau, A. Sobkowski, G. Theraulaz, and J. Deneubourg, "Adaptive task allocation inspired by a model of division of labor in social insects," in *Proc. BCEC*, no. 8, 1997, pp. 36–45.
- [25] D. Teruya, B. Indurkha, T. Maksaki, and H. Nakajo, "Autonomous distributed system based on behavioral model of social insects," in *Proc. Int. Conf. Parallel Distrib. Process. Techn. Appl.*, 2018, pp. 289–295.
- [26] Z. Ding, Y. Huang, H. Yuan, and H. Dong, "Introduction to reinforcement learning," in *Deep Reinforcement Learning*. Singapore: Springer, 2020, pp. 47–123.
- [27] E. Bonabeau, "Fixed response thresholds and the regulation of division of labor in insect societies," *Bull. Math. Biol.*, vol. 60, no. 4, pp. 753–807, Jul. 1998.
- [28] G. Theraulaz, E. Bonabeau, and J.-N. Deneubourg, "Response threshold reinforcements and division of labour in insect societies," *Proc. Roy. Soc. London B, Biol. Sci.*, vol. 265, no. 1393, pp. 327–332, Feb. 1998.
- [29] P. Anderson and A. Bose, "Stability simulation of wind turbine systems," *IEEE Trans. Power App. Syst.*, vols. PAS-102, no. 12, pp. 3791–3795, Dec. 1983.
- [30] L. Wang, D.-J. Lee, W.-J. Lee, and Z. Chen, "Analysis of a novel autonomous marine hybrid power generation/energy storage system with a high-voltage direct current link," *J. Power Sources*, vol. 185, no. 2, pp. 1284–1292, Dec. 2008.
- [31] S. Mousavi and M. Nikdel, "Various battery models for various simulation studies and applications," *Renew. Sustain. Energy Rev.*, vol. 32, pp. 477–485, Apr. 2014.
- [32] M. Soltani, F. Moradi Kashkooli, M. Souri, B. Rafiei, M. Jabarifar, K. Gharali, and J. S. Nathwani, "Environmental, economic, and social impacts of geothermal energy systems," *Renew. Sustain. Energy Rev.*, vol. 140, Apr. 2021, Art. no. 110750.
- [33] S. J. Zarrouk and H. Moon, "Efficiency of geothermal power plants: A worldwide review," *Geothermics*, vol. 51, pp. 142–153, Jul. 2014, doi: 10.1016/J.GEOTHERMICS.2013.11.001.
- [34] E. Espe, V. Potdar, and E. Chang, "Prosumer communities and relationships in smart grids: A literature review, evolution and future directions," *Energies*, vol. 11, no. 10, p. 2528, Sep. 2018.
- [35] M. Tesfaye, B. Khan, O. P. Mahela, H. H. Alhelou, N. Gupta, M. Khosravy, T. Senjyu, and J. M. Guerrero, "Analysing integration issues of the microgrid system with utility grid network," *Int. J. Emerg. Electric Power Syst.*, vol. 22, no. 1, pp. 113–127, Feb. 2021.
- [36] P. Domański, *Control Performance Assessment: Theoretical Analyses and Industrial Practice*. Springer, 2020.
- [37] D. Diagne and P. Lauret, "Outputs and error indicators for solar forecasting models," in *Proc. World Renewable Energy Forum*, May 2012, pp. 13–17.
- [38] B. Alagoz, A. Kaygusuz, and A. Karabiber, "A user-mode distributed energy management architecture for smart grid applications," *Energy*, vol. 44, pp. 167–177, Aug. 2012.
- [39] J. Aguilar, M. Cerrada, and F. Hidrobo, "A methodology to specify multi-agent systems," in *Proc. KES Int. Symp. Agent Multi-Agent Syst., Technol. Appl.*, in Lecture Notes in Computer Science, vol. 4496, 2007, pp. 92–101.

1134 [40] J. Aguilar, I. Bessemel, M. Cerrada, F. Hidrobo, and F. Narciso, "Una
1135 metodología para el modelado de sistemas de ingeniería orientado a
1136 agentes inteligencia artificial," *Revista Iberoamericana de Inteligencia*
1137 *Artif.*, vol. 12, no. 38, pp. 39–60, 2008.

1138 [41] M. N. Alam, S. Chakrabarti, and X. Liang, "A benchmark test system
1139 for networked microgrids," *IEEE Trans. Ind. Informat.*, vol. 16, no. 10,
1140 pp. 6217–6230, Oct. 2020.



MARCEL SIMEÓN GARCÍA MEDINA received the Electronic Engineer degree from Universidad Nacional Experimental del Táchira (UNET), in 2005, and the Magister Scientiarum degree in research and development project management from Rafael Belloso Chacín University (URBE), in 2011. He was an Integrator of industrial automation systems and a Maintenance Supervisor of SCADA Platform, Petróleos de Venezuela S. A. (PDVSA), for 13 years. He is currently an Instructor Professor with the UNET. His research interests include robotics, industrial automation, and artificial intelligence.



JOSE AGUILAR (Member, IEEE) received the Systems Engineer degree from the Universidad de los Andes, Mérida, Venezuela, in 1987, the M.Sc. degree in computer science from Université Paul Sabatier-France, in 1991, the Ph.D. degree in computer science from Université René Descartes-France, in 1995, and the Postdoctoral degrees from the Department of Computer Science, University of Houston, in 2000, and the Laboratoire d'analyse et d'architecture des systèmes (LAAS), CNRS, Toulouse, France, in 2011. He is currently a Full Professor at the Department of Computer Science, Universidad de los Andes. He is also a member of the Mérida Science Academy and the IEEE CIS Technical Committee on Neural Networks. He has a Marie Skłodowska-Curie Fellowship at the University of Alcalá. He has published more than 600 articles and ten books, in the field of parallel and distributed computing, computer intelligence, and science and technology management. His research interests include artificial intelligence, semantic mining, big data, emerging computing, and intelligent environments.



MARIA D. RODRÍGUEZ-MORENO received the Ph.D. degree (Hons.) in computer science from the Universidad de Alcalá (UAH), Madrid, Spain. She has been a Full Professor at UAH, since 2018. Since 2021, she has been collaborating with TNO (The Netherlands) as a Senior Scientist. She has published over 100 journals, books, and conference papers. Her research interests include artificial intelligence (AI), in particular AI planning and scheduling, evolutionary computation, machine learning, and intelligent execution applied to real applications, such as aerospace, robotics, and cybersecurity or energy management. She has served in the program committee for several international AI conferences and a reviewer for international journals. She received the European Ph.D. Award of Best Doctoral Dissertation.

• • •